Physics – Uspekhi **62** (3) 282 – 288 (2019)

CONFERENCES AND SYMPOSIA

PACS numbers: **42.65. – k**, 42.65.Jx, 42.65.Ky, 42.65.Re, 52.38.Hb

Light bullet dynamics in uniform dielectrics

(50th anniversary of the Institute of Spectroscopy, Russian Academy of Sciences)

S V Chekalin, V O Kompanets, A E Dormidonov, V P Kandidov

DOI: DOI: https://doi.org/10.3367/UFNe.2018.06.038419

Contents

Abstract. Experiments and numerical simulations performed jointly by the Institute of Spectroscopy, Russian Academy of Sciences, and Lomonosov Moscow State University have shown that unlike solitons in guiding structures, the light bullet, a wave packet compressed to the extreme in space and time in the bulk of a transparent dielectric, is a short-lived formation whose free path is no more than several hundred micrometers. The supercontinuum spectrum generated by a light bullet experiences superbroadening, and an isolated anti-Stokes wing emerges if the bullet is compressed to the state of a wave packet close to the single-cycle one, and a plasma channel develops. These findings have been confirmed by numerical simulations and experiments demonstrating periodic density modulation of the color centers induced in LiF, which occurs due to the difference between the wave packet envelope and frequency-carrier velocities in a medium.

Keywords: filamentation, light bullets, anomalous group velocity dispersion, supercontinuum

1. Introduction

The term light bullet (LB) was introduced for self-consistent nonlinear excitations with a light field highly localized in space and time. The concept of LB formation due to the combined and consistent compression of laser radiation in space and time during the self-action of a wave packet in a dispersive medium with cubic nonlinearity was formulated in [1] by analyzing quasi-optic equations in the aberrationless axial approximation [2]. At present, studies in this field are developing in at least two directions. One is devoted to the formation of stable LBs (three-dimensional solitons), i.e., self-consistent nonlinear excitations localized in space and time and propagating over large distances without spreading or noticeable distortions in 'guiding' structures with a nonlinearity fundamentally different from a purely cubic nonlinearity [3]. The realization of such self-consistent structures in a stable state is one of the most experimentally complicated and so far unsolved problems of modern nonlinear optics.

Our study falls within the other area, in which, beginning with the first work on self-focusing and then filamentation [4], homogeneous and isotropic media with cubic nonlinearity are considered, and light field localization occurs in the bulk of the medium. In this case, the role of a guiding structure is played by a filament formed during the propagation of a high-power femtosecond laser pulse in a nonlinear dispersive medium. Filamentation is light field localization during the propagation of a high-power laser pulse in transparent dielectrics maintained by the dynamic balance of Kerr self-focusing in the medium and defocusing in the induced laser plasma in the presence of diffraction and material dispersion. Because of the high energy concentration in a filament, its considerable length. and the stability of its parameters, the nonlinear optical interaction of a light field with the medium becomes stronger and the spatiotemporal and spectral parameters of radiation are considerably transformed. Filamentation leads to the superbroadening of the frequency and angular spectra of a femtosecond pulse, i.e., supercontinuum (SC) generation.

The material dispersion of the medium strongly affects filament formation and the spatiotemporal radiation intensity distribution during filamentation. In the region of normal group velocity dispersion (GVD), the pulse decomposes into subpulses. In the region of zero GVD, the trailing edge of the pulse defocused in a self-induced laser plasma undergoes multiple Kerr self-focusing. Under anomalous GVD conditions, light bullets occur in the filament in the form of extremely compressed wave packets with the light field strongly localized in space and

S V Chekalin [(1,*)], **V O Kompanets** [(1)], **A E Dormidonov** [(1,2)], **V P Kandidov** [(1,2)]
[(1)] Institute of Spectroscopy, Russian Academy of Sciences, ul. Fizicheskaya 5, 108840 Troitsk, Moscow, Russian Federation
[(2)] Faculty of Physics, Lomonosov Moscow State University, Leninskie gory 1, bld 2, 119991 Moscow, Russian Federation
E-mail: * chekalin@isan.troitsk.ru

Received 15 August 2018
Uspekhi Fizicheskikh Nauk **189** (3) 299 – 305 (2019)
DOI: https://doi.org/10.3367/UFNr.2018.06.038419
Translated by M N Sapozhnikov; edited by A M Semikhatov

time. As the pulse energy is increased, a quasiperiodic train of light bullets appears [5].

The problem of obtaining three-dimensional solitons in a transparent medium remains open so far because they are unstable and can collapse or decompose [6]. Nevertheless, after the development of femtosecond lasers emitting in the mid-IR spectral range, where the GVD of many transparent dielectrics is anomalous (which is necessary for LB formation), studies of pulse filamentation in this spectral range began. Because the threshold self-focusing power for filamentation to develop increases proportionally to the wavelength squared, experiments in the near and mid-IR range require a considerable increase in the laser pulse energy. The extremal localization of the light field in space and time down to a few wavelengths in diameter and one optical cycle in duration accompanying the propagation of a high-peak-intensity wave packet in a homogeneous medium in the case of anomalous GVD results in the formation of LBs. This is in turn related to SC generation in the spectral range from the UV region to the mid-IR region, with an isolated anti-Stokes wing formed in the visible range.

The peak powers of femtosecond pulses emitted by modern lasers can reach a few petawatts, corresponding to peak intensities at the level of $10^{13}-10^{14}$ W cm^{-2}. Under these conditions, the nonlinear contribution to the refractive index of a medium becomes considerable, and nonlinear self-action effects inevitably accompanying the propagation of high-intensity radiation in a transparent medium considerably change the spatiotemporal and spectral parameters of the propagating pulses. Therefore, with the advent of lasers emitting subterawatt ultrashort pulses in the mid-IR spectral range [7], the study of the ultrafast dynamics of extremely compressed wave packets one to two optical cycles in duration with the transverse size of the order of the wavelength and the peak intensity up to 10^{14} W cm^{-2} propagating in isotropic transparent dielectrics becomes quite urgent for extremal laser optics.

One of the key problems in this field is studying the dynamics of wave packets and determining the main energy dissipation channels. This will allow finding similarity parameters and scaling the results obtained to various media, in particular, gaseous media.

2. Registration of light bullets and accompanying supercontinuum emission

Light bullets about two optical cycles in duration were first observed in our paper [8] by measuring their autocorrelation function during the filamentation of femtosecond pulses in a fused silica in the anomalous dispersion region at 1900 nm. As the incident pulse energy was increased, the second and third LBs appeared (Fig. 1), in good agreement with numerical calculations [9, 10]. Estimates of the plasma channel length in these experiments showed that the LB mean free path did not exceed a few millimeters. Therefore, the statement of the authors of [11] that the mean free path of LBs reached a few centimeters under the same filamentation conditions, which was reproduced in some subsequent studies [12–14], proved to be somewhat unexpected. This conclusion is mainly based on photographs of a long luminous plasma channel and scattered SC emission track detected through the side surface of a sample. This track was interpreted as the luminescence of silica observed during the propagation of a long-lived soliton (LB) over a few

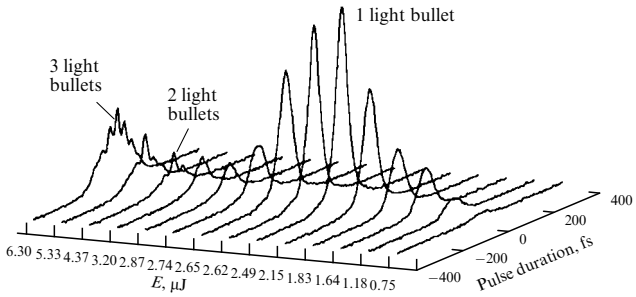

Figure 1. Autocorrelation functions of LBs in fused silica recorded upon increasing the acting pulse energy (μJ).

centimeters in the sample. According to such experiments, the LB mean free path in sapphire was 10 mm [12], and the mean free path in fused silica was estimated as a few centimeters in [11], which considerably exceeds the values obtained in [8, 15].

Along with the LB lifetime (or the free path), the question of the LB nature and the nature of accompanying SC emission is very important and is still being discussed. Some researchers found this phenomenon analogous to so-called 'rogue waves' [16], which have been recently documented to exit in the world's ocean, albeit without an explanation of their nature. Emission appearing in the visible SC band was treated similarly to the generation of high frequencies in fiber converters due to resonance energy exchange between the soliton and a dispersion wave induced by the higher-order dispersion (resonance emission). The authors of [16] observed a strong scatter in the visible SC band energy generated during the LB formation in sapphire, and they assume that this confirms their concept.

An analysis of our experiments [17, 18] sheds light on both these questions. To record the luminous plasma channel and scattered SC tracks, the signal accumulation for a fairly large number of laser pulses is fundamentally necessary. The same problem is also inherent in the 3D imaging method used by a number of foreign groups [19]. The shot-to-shot irreproducibility of laser pulse parameters considerably distorts the information obtained. Figure 2 demonstrates this with the example of luminous tracks recorded in fused silica for different energies of exciting laser pulses corresponding to

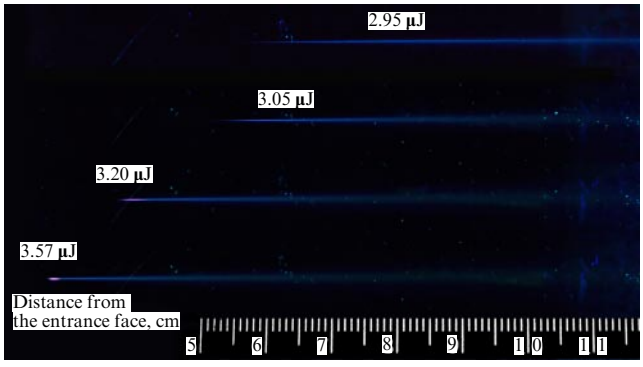

Figure 2. (Color online.) Images (for 10 thousand pulses) of the SC emission scattered in a sample and emission of plasma generated in fused silica by a 1900 nm, 50 fs laser pulse focused with a lens with a focal length of 0.585 m on the entrance face of the sample onto a spot 135 μm in diameter (pulse energies and scale are shown in the figure).

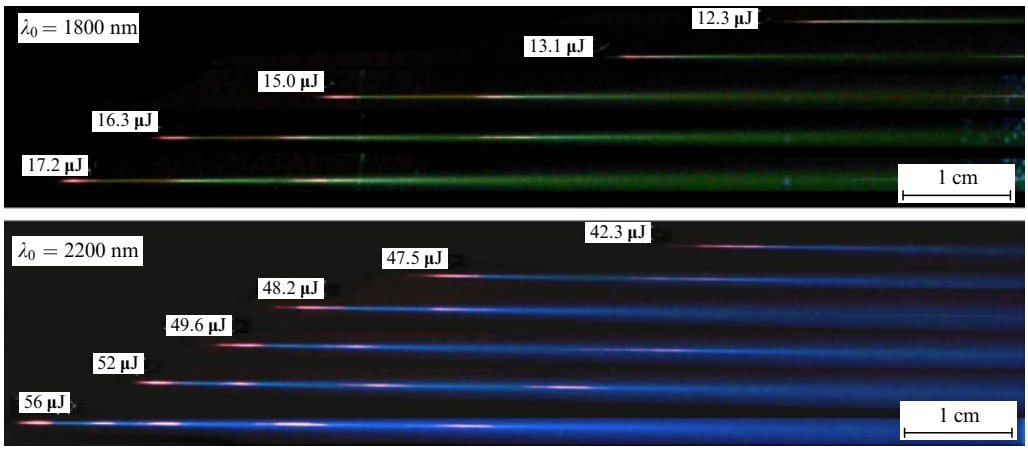

Figure 3. (Color online.) Tracks of plasma channels and scattered SC emission recorded in fused silica upon filamentation of femtosecond pulses with different energies at different wavelengths.

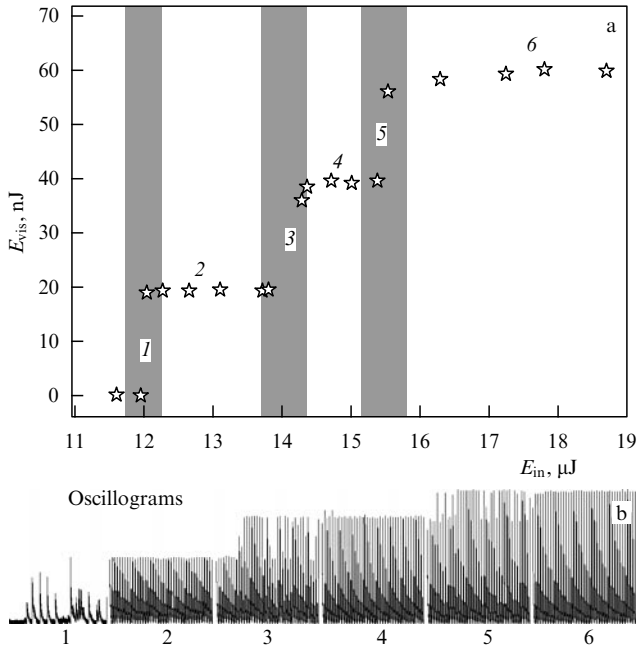

Figure 4. (a) Dependence of the energy E_{vis} of the visible SC on the 1800 nm input pulse energy E_{in}. (b) Oscillograms of a photodiode signal measuring the energy of each pulse in the visible region. Numbers *1*, *3*, and *5* denote the vicinities of threshold energies shown in gray in Fig. 4a at which the first, second, and third plasma channels appear and the respective LBs appear in the filament.

the formation of the first LB in a filament. The scattered SC emission appears at an energy of 2.95 μJ, corresponding to a threshold peak power of 53 MW for LB formation. We can see that for a laser pulse energy close to the filamentation threshold, we have failed to record a plasma channel, even after exposure to 10 thousand pulses, whereas the length of the scattered SC emission track in this case is maximal, exceeding 5 cm. This is related to a large scatter in start points at the filamentation threshold. The stabilization of the start point position with increasing energy allows recording a plasma channel whose length, as that of the scattered SC track, noticeably decreases upon exceeding the stable formation threshold of the first LB (see Fig. 2).

Photographs of color tracks appearing in fused silica upon increasing the pulse energy during the formation of one, two, three, etc. LBs (up to seven, corresponding to the number of plasma channels appearing) have revealed tracks more than 10 cm in length (Fig. 3). But as the excitation wavelength was tuned from the near-IR to the mid-IR range, their color changed according to the color of the visible SC band. This shows that the color tracks are related not to the luminescence of a sample but to the SC scattering in it and therefore they in no way characterize the LB mean free path. The measurement of the SC anti-Stokes wing energy showed that the formation of an LB in the femtosecond filament is accompanied by an outburst of a discrete energy portion in the visible SC band. The dependence of the visible SC energy on the laser pulse energy has a step-like shape, the appearance of each next step being related to the formation of the next LB in the filament. Each bullet in the LB sequence emits the same portion of the visible SC energy. It is important that in contrast to [16], this energy detected in each laser pulse remains invariable even upon increasing the laser pulse energy until the formation of the next LB (Fig. 4). Hence, the appearance of the isolated SC anti-Stokes wing observed for the first time in [20] and then investigated in more detail in [21] is related to LB formation [8]. Based on the experimental data obtained and earlier spectral measurements, we conclude that the LB energy is almost completely transformed to the entire SC band, being the main LB dissipation channel.

3. Measurement of the light bullet free path by the laser coloration method

Measuring the LB free path is of great practical interest, in particular, for problems in atmospheric optics, where the results obtained for solid dielectrics can be scaled. The laser coloration method [22–24] allows performing measurements, first, without signal accumulation, i.e., using only a single laser pulse, which completely eliminates measurement error caused by scatter in the pulse energy and, second, in the complete absence of parasitic SC, conic, and plasma channel emissions. The LB appearance and development dynamics during filamentation of single mid-IR femtosecond pulses in LiF is studied by the change in the density of long-lived color centers (CCs) appearing in the light field due to multiphoton processes in the LBs produced. In this case, long-lived

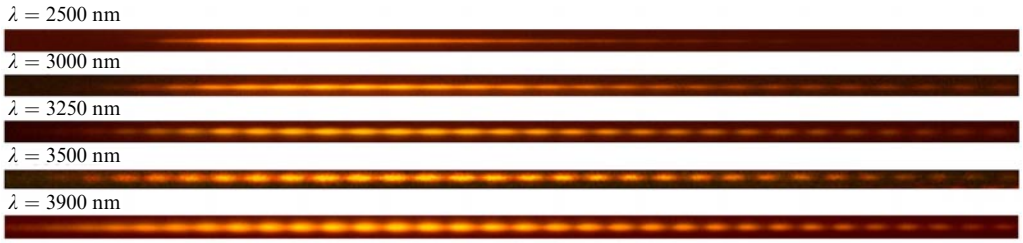

Figure 5. Luminescence tracks of CCs induced in LiF upon single-pulse filamentation of femtosecond pulses at wavelengths in the range 2500–3900 nm.

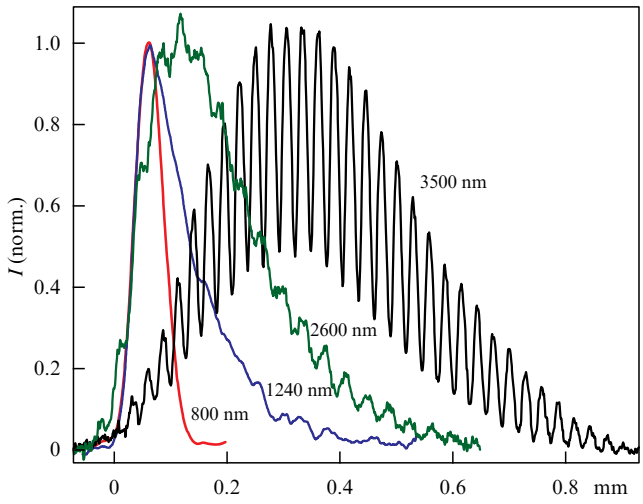

Figure 6. Normalized CC luminescence densities recorded after single-pulse filamentation at various wavelengths (shown in the figure) as functions of the distance from the filament start point (mm).

structures consisting of CCs produced by only a single laser pulse can be easily recorded and studied by posterior illumination of the sample by a cw laser in their absorption band near 450 nm. This allows detailed studies of the three-dimensional structure of the LB optical field over its entire free path inside a material with a spatial resolution better than 1 μm (determined exclusively by the resolving power of the microscope used).

Photographs of the luminescence of CCs induced in LiF upon single-pulse filamentation of femtosecond pulses in the region of a strong anomalous GVD are shown in Fig. 5. Figure 6 presents the luminescence density profiles for CCs induced by laser pulses at wavelengths ranging in the mid- and near-IR bands between 800 and 3500 nm. It can be seen that upon excitation by a single pulse at a wavelength corresponding to the normal GVD in LiF, the length of the region with the high light field intensity (i.e., the filament length) increases with the wavelength from 70 μm at 800 nm to 120 μm at 1240 nm (the zero GVD region) and then to 250 μm at 2100 nm (the weak anomalous GVD region). In this case, the profiles of the CC structures induced in the filament are rather smooth. For quite large anomalous GVD (beginning at 2600 nm), a regular CC structure appears in profiles, which directly reproduces the influence of the absolute phase of the light field of an extremely compressed wave packet on the nonlinear optical interaction (see Figs 5 and 6). It is well known that during the propagation of a single-cycle light pulse in a dispersive medium, the cyclic period modulation of the maximal amplitude of the pulse light field occurs due to the difference between the velocities of the pulse envelope and its carrier frequency [25]. This process is inherent only in single-cycle pulses; the modulation effect almost vanish as the number of periods increases. Therefore, the appearance of a regular modulation of the density profile of CCs induced during filamentation in LiF (see Fig. 5) indicates the formation of a single-cycle LB.

The LB free path somewhat increases with increasing wavelength (see Fig. 6), but, unlike data in [11, 12], does not exceed a few hundred micrometers, corresponding to a lifetime of the order of several picoseconds. The track appearance does not change with increasing the laser pulse energy from the filament appearance threshold to the appearance of a second LB with the same structure as that of the first LB, indicating the bullet robustness [26].

4. Dynamics of light bullet formation and supercontinuum emission. Some numerical simulation results

The light field evolution during the formation of a single-cycle LB and its propagation in LiF was analyzed by solving the unidirectional propagation equation [27], which most completely describes the filamentation of a femtosecond laser pulse, using the computer code developed in [28]. A similar picture of the pulse and its spectrum transformation was obtained in [29] for filamentation of 4 μm radiation in air. The problem was formulated taking the diffraction and dispersion of a wave packet, Kerr self-focusing, the photo- and avalanche ionization of the medium, light defocusing, and absorption in the induced plasma into account. As the initial condition in simulations, a wave packet was specified with a Gaussian distribution of the electric field strength amplitude in time and space, with the parameters corresponding to experimental data. These parameters, 100 fs FWHM duration of the wave packet, 100 μm beam diameter, 20 μJ beam energy, and 3500 nm central wavelength of the beam, correspond to the peak power of about 1.5 times the critical self-focusing power in LiF. The calculated temporal profiles of the light field in the LB in Figs 7 and 8 are presented in the local pulse reference frame $\tau = t - z/v_g$, where v_g is the pulse group velocity. Figures 7a, d present the initial temporal profile of the light field and the pulse spectrum on the beam axis.

Under the action of the Kerr nonlinearity and anomalous GVD, the light pulse is compressed in space and time, and the light field amplitude increases by several times (Fig. 7 b). Due to the nonlinear phase modulation, the pulse spectrum begins to broaden (Fig. 7e). Further pulse compression to a single-cycle LB leads to an increase in the light field intensity above 10^{14} W cm^{-2} (Fig. 7c) and the beginning of avalanche ionization and the generation of excitons in the medium. At

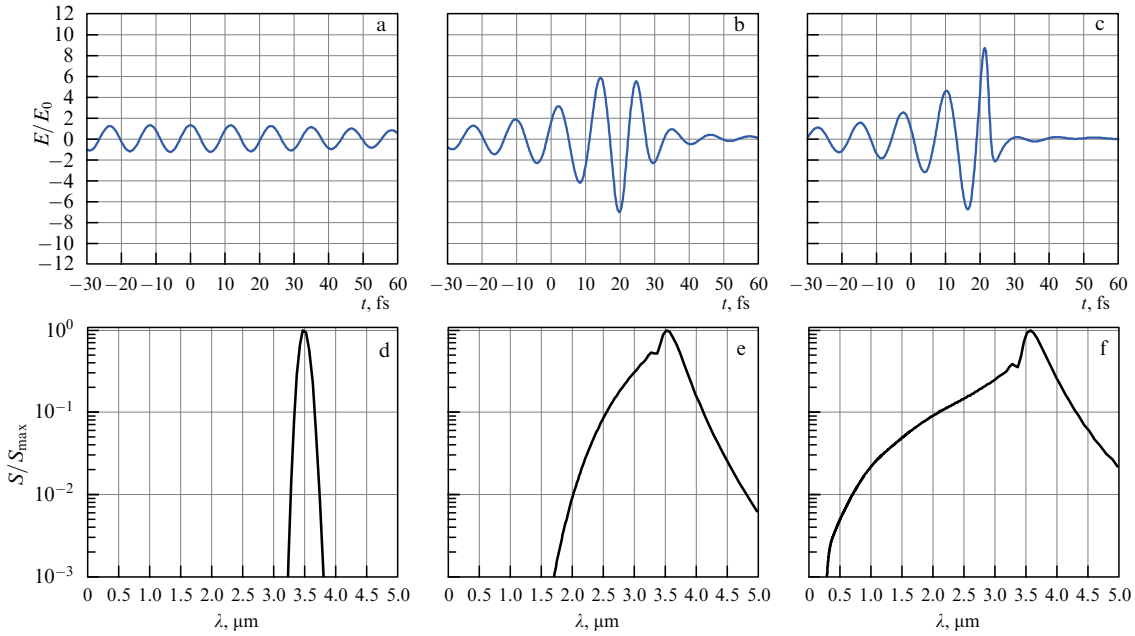

Figure 7. (a–c) Light field profiles on the wave packet axis and (d–f) corresponding spectra at several distances z from the entrance to the medium: (a, d) $z = 0$: the initial wave packet; (b, e) $z = 6.64$ mm; (v, f) $z = 6.72$ mm: the LB formation stage.

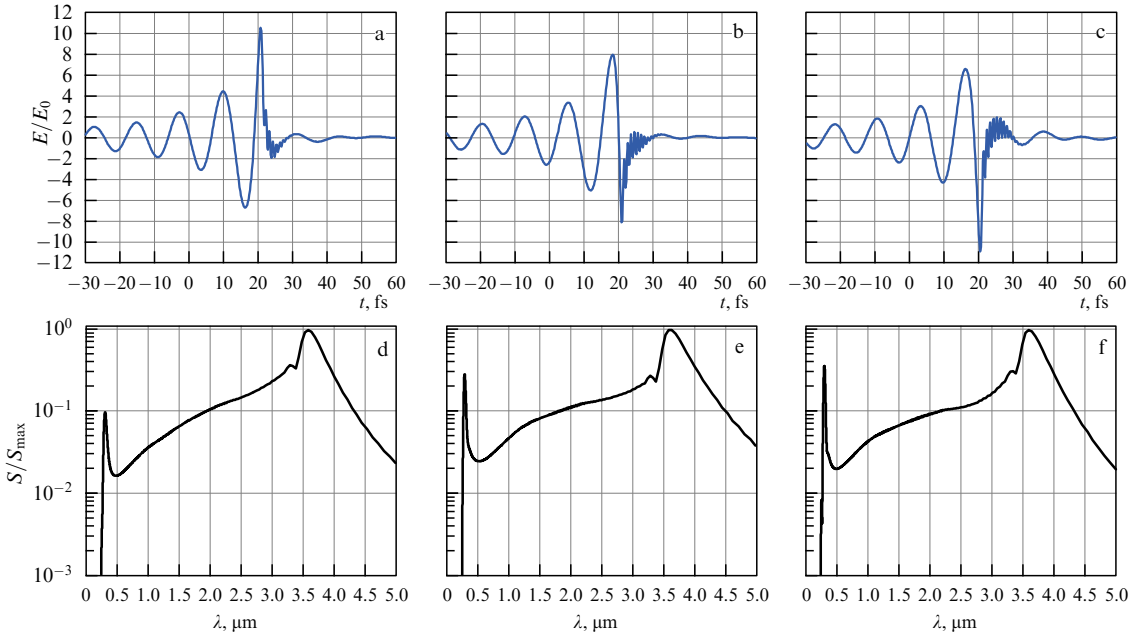

Figure 8. (a–c) Light field profiles on the LB axis and (d–f) corresponding spectra at several distances z from the entrance to the medium: (a, d) $z = 6.778$ mm: the maximum of the LB wave packet envelope coincides with the carrier wave maximum; (b, e) $z = 6.795$ mm: the maximum of the LB wave packet envelope coincides with the carrier wave zero; (c, f) $z = 6.808$ mm: the maximum of the LB wave packet envelope coincides with the carrier wave minimum.

this instant, the spectrum becomes monotonically broadened in the anti-Stokes region and covers the entire visible range, with SC generation taking place (Fig. 7f). The SC short-wavelength boundary is determined by the ratio of the gap width of the medium to the photon energy at the central wavelength of the pulse [30].

Light field defocusing in the plasma produced leads to the shortening of the pulse trailing edge (Fig. 8a). The FWHM LB duration becomes less than 10 fs, which is about 10% of the initial pulse duration. Because of the difference between the phase and group velocities, the light wave moves faster than the wave packet envelope. We can see that for $z_1 = 6.778$ mm (Fig. 8a), the maximum of the LB wave packet envelope coincides with the light wave maximum, and for $z_2 = 6.795$ mm (Fig. 8b), the light wave is displaced by a quarter of the period, and the resulting peak amplitude of the light field strength in the LB decreases by more than 20%. For $z_3 = 6.808$ mm (Fig. 8c), the maximum of the LB wave packet envelope coincides with the light wave minimum. The modulus of the electric field strength amplitude again

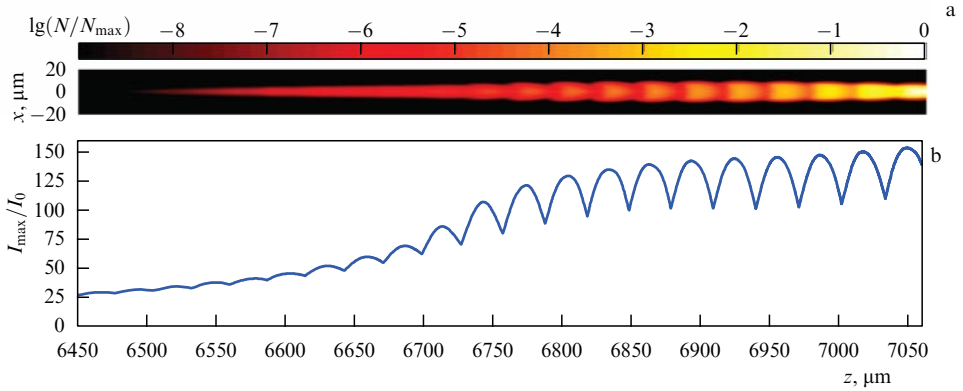

Figure 9. Calculated electron density distribution (integrated over one of the transverse coordinates) in a medium during the propagation of a single-cycle LB (a) and the corresponding maximum LB intensity (b).

becomes maximal. Thus, during the propagation of an LB as a single-cycle wave packet, the field amplitude periodically changes due to the difference between the group and phase velocities.

Such oscillations of the peak amplitude of the electric field with a period of about 30 μm continue during the LB lifetime and were recorded in experiments as a regular structure consisting of CCs (see Fig. 5). Because of the multiphoton CC generation process involving about 30 photons, a change in the electric field amplitude by 20% leads to a reliably recorded CC density modulation during the LB propagation [23, 24]. Figure 9 shows the calculated plasma density distribution in a channel during the propagation of a single-cycle LB, which is consistent with experimental measurements of the CC density in LiF (see Fig. 5).

The LB spectrum exhibits an isolated anti-Stokes peak (Figs 8d–f) whose position is determined by the constructive interference condition, from which the dispersion equation follows [31]. High-frequency light-field oscillations at the frequency corresponding to the short-wavelength SC maximum are observed at the trailing edge of temporal LB profiles (Figs 8a–c).

5. Conclusions

The LB is the result of the self-organization of a light-field wave packet in a nonlinear dispersive medium in the case of anomalous GVD. Unlike solitons in guiding structures, the LB in a transparent dielectric is a short-lived entity with a free path of a few hundred micrometers. The LB mean free path is uniquely and reliably determined in the single-pulse filamentation regime by the laser coloration method, which is free from the errors of other methods relying on signal accumulation in the multipulse measurement regime. The LB formed in a transparent dielectric upon filamentation of a femtosecond pulse in the case of anomalous GVD is compressed into a single-cycle wave packet. The single-cycle duration of the LB is confirmed experimentally using the laser coloration method recording the induced structure with CC density modulation in LiF appearing due to the periodic change in the light field amplitude caused by the difference between the phase velocity of the light field and the group velocity of the wave packet envelope during LB propagation. It has been shown experimentally and numerically that SC superbroadening and the appearance of an isolated anti-Stokes wing in it occur upon LB compression to a single-cycle wave packet and the formation of a plasma channel. In this case, the LB free path and lifetime are determined by energy losses due to the bullet energy conversion to broadband SC energy and absorption in plasma.

Upon filamentation of near-IR radiation at a wavelength lying in the normal GVD region, the wave packet compression in time is absent, a single-cycle LB is not formed, and the CC density induced in LiF changes monotonically along the filament.

Acknowledgments

Experiments were performed using the unique Multipurpose Femtosecond Laser Diagnostic Facility at the Institute of Spectroscopy, RAS. The study was supported by the Russian Science Foundation (project no. 18-12-00422).

References

1. Silberberg Y *Opt. Lett.* **22** 1282 (1990)
2. Akhmanov S A, Sukhorukov A P, Khokhlov R V *Sov. Phys. Usp.* **10** 609 (1968); *Usp. Fiz. Nauk* **93** 19 (1967)
3. Kartashov Y V, Malomed B A, Torner L *Rev. Mod. Phys.* **83** 247 (2011)
4. Chekalin S V, Kandidov V P *Phys. Usp.* **56** 123 (2013); *Usp. Fiz. Nauk* **183** 133 (2013)
5. Smetanina E O, Dormidonov A E, Kandidov V P *Laser Phys.* **22** 1189 (2012)
6. Kuznetsov E A, Dias F *Phys. Rep.* **507** 43 (2011)
7. Ališauskas S et al., in *CLEO 2013, QELS-Fundamental Science, 9 June–14 June 2013, San Jose, CA, USA* (OSA Technical Digest) (Washington, DC: Optical Society of America, 2013) QW1E.6, https://doi.org/10.1364/CLEO_QELS.2013.QW1E.6
8. Smetanina E O et al. *Laser Phys. Lett.* **10** 105401 (2013)
9. Smetanina E O et al. *Quantum Electron.* **42** 913 (2012); *Kvantovaya Elektron.* **42** 913 (2012)
10. Bergé L, Skupin S *Phys. Rev. E* **71** 065601(R) (2005)
11. Durand M et al. *Phys. Rev. Lett.* **110** 115003 (2013)
12. Majus D et al. *Phys. Rev. Lett.* **112** 193901 (2014)
13. Gražulevičiūtė I et al. *J. Opt.* **18** 025502 (2016)
14. Brée C et al. *Phys. Rev. Lett.* **118** 163901 (2017)
15. Chekalin S V et al. *Quantum Electron.* **43** 326 (2013); *Kvantovaya Elektron.* **43** 326 (2013)
16. Roger T et al. *Phys. Rev. A* **90** 033816 (2014)
17. Chekalin S V et al. *Quantum Electron.* **45** 401 (2015); *Kvantovaya Elektron.* **45** 401 (2015)
18. Chekalin S V et al. *J. Phys. B* **48** 094008 (2015)
19. Potenza M A C et al. *Opt. Commun.* **229** 381 (2004)
20. Saliminia A, Chin S L, Vallée R *Opt. Express* **13** 5731 (2005)
21. Smetanina E O et al. *Opt. Lett.* **38** 16 (2013)

22. Martynovich E F et al. *Quantum Electron*. **43** 463 (2013); *Kvantovaya Elektron*. **43** 463 (2013)
23. Kuznetsov A V et al. *Quantum Electron*. **46** 379 (2016); *Kvantovaya Elektron*. **46** 379 (2016)
24. Chekalin S V et al. *Laser Phys. Lett*. **13** 065401 (2016)
25. Xu L et al. *Opt. Lett*. **21** 2008 (1996)
26. Chekalin S V et al. *Quantum Electron*. **48** 372 (2018); *Kvantovaya Elektron*. **48** 372 (2018)
27. Kolesik M, Moloney J V *Phys. Rev. E* **70** 036604 (2004)
28. Fedorov V Yu et al. *Phys. Rev. Lett*. **117** 043902 (2016)
29. Panagiotopoulos P et al. *Nature Photon*. **9** 543 (2015)
30. Kandidov V P, Kompanets V O, Chekalin S V *JETP Lett*. **108** 287 (2018); *Pis'ma Zh. Eksp. Teor. Fiz*. **108** 307 (2018)
31. Dormidonov A E et al. *JETP Lett*. **104** 175 (2016); *Pis'ma Zh. Eksp. Teor. Fiz*. **104** 173 (2016)